

# Single crystal solution growth and studies of $(\text{Fe}_{1-x}\text{Co}_x)_2\text{B}$

Kelly J. Neubauer,\* Peter Klavins, Jackson Badger, and Valentin Taufour†

*Department of Physics, University of California, Davis*

(Dated: November 8, 2017)

Single crystals have clear axes that allow for studies of the directional dependence of magnetic properties. Single crystals of  $(\text{Fe}_{1-x}\text{Co}_x)_2\text{B}$  were produced using a solution growth method for Co doping levels ranging from 11-17%.  $(\text{Fe}_{1-x}\text{Co}_x)_2\text{B}$  crystals exhibit a spin reorientation transition at temperatures between 5 and 300 K when  $x = 11 - 13\%$ . Near the spin reorientation temperature, an inverse magneto-caloric effect was observed for  $x_{\text{nominal}} = 11\%$  when a magnetic field was applied along the  $c$ -axis of the crystal. No magneto-caloric effect was observed when a magnetic field was applied perpendicular to the  $c$ -axis.

## I. INTRODUCTION

Many different materials are studied by condensed matter physicists including nanomaterials, thin films, polycrystals and single crystals. These materials each provide opportunities for particular studies and applications. We study single crystals which are unique in having clear axes, no grain boundaries, and small sample sizes. The existence of clear axes is relevant to our studies of a spin reorientation transition between axes and its resulting magneto-caloric effect.

The magneto-caloric effect is the absorption or emission of heat by a magnetic material under the application or removal of a magnetic field. This is observed as either a change in temperature under adiabatic conditions or as a change in entropy under isothermal conditions ( $\Delta S_{\text{iso}}$ ).

The study of materials exhibiting a magneto-caloric effect is important for the understanding of magnetism and condensed matter physics in addition to their technological applications. [1] Technologies based on the magneto-caloric effect replace conventional compressing and decompressing of gases with magnetization and demagnetization in devices such as refrigerators, air conditioners, and freezers. This technology provides a quieter, more energy efficient, and more environmentally friendly alternative for cooling devices. [2] Significant work has been done in recent years to study materials that exhibit a large magneto-caloric effect near room temperature for these applications.

The magneto-caloric effect of  $(\text{Fe}_{1-x}\text{Co}_x)_2\text{B}$  is associated with a spin reorientation at a transition temperature  $T_{sr}$ . At temperatures greater than  $T_{sr}$ , magnetic moments are parallel to the  $c$  axis. At temperatures less than  $T_{sr}$ , magnetic moments are perpendicular to the  $c$ -axis.  $T_{sr}$  is tunable with the proper choice of doping level ( $x_{\text{nominal}}$ ), the percentage of Fe replaced with Co.

$(\text{Fe}_{1-x}\text{Co}_x)_2\text{B}$  is a metal as well as a ferromagnet. Above its Curie temperature,  $T_C$ , magnetic spins are randomly oriented. As temperature is reduced below  $T_C$ , domains form and align until all spins are oriented along

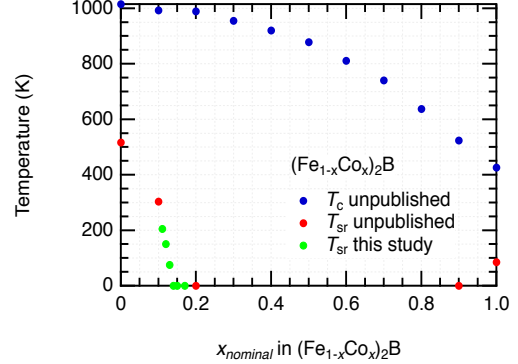


FIG. 1. Variation in Curie temperature,  $T_C$ , and spin reorientation temperature,  $T_{sr}$ , as a function of Co doping level,  $x$ , in  $(\text{Fe}_{1-x}\text{Co}_x)_2\text{B}$ .  $T_{sr}$  between 0.1 and 0.2 were observed between 0 and 300 K, the focus range of this study. This figure includes unpublished Taufour group data in addition to values measured in this study [4] (seen in green.)

one axis.  $(\text{Fe}_{1-x}\text{Co}_x)_2\text{B}$  has a  $T_C$  near 1000 K, which is tunable by Co doping as seen in Figure 1.

The crystal structure of  $\text{Fe}_2\text{B}$  is tetragonal with  $a = b = 5.12040\text{\AA}$ ,  $c = 4.25880\text{\AA}$ , and  $\alpha = \beta = \gamma = 90^\circ$ . The space group is  $I 4/m c m$ . Axes  $a$  and  $b$  are equivalent and are the easy plane for spin alignment when  $T < T_{sr}$ . Spins align with the  $c$  axis when  $T > T_{sr}$ .

Previous studies of  $(\text{Fe}_{1-x}\text{Co}_x)_2\text{B}$  have not included measurements of its magneto-caloric effect. The goal of this study was to observe a magneto-caloric effect and inverse magneto-caloric effect as a magnetic field was applied along different axes of  $(\text{Fe}_{1-x}\text{Co}_x)_2\text{B}$  single crystals. This study would lead to further understanding of the  $(\text{Fe}_{1-x}\text{Co}_x)_2\text{B}$  material as well as the magneto-caloric effect and its potential for application.

## II. EXPERIMENTAL TECHNIQUES

$(\text{Fe}_{1-x}\text{Co}_x)_2\text{B}$  ( $x = 0.11 - 0.17$ ) compounds were synthesized by solution crystal growth. The stoichiometry was chosen considering binary phase diagrams for Fe-B and Co-B [3]. The Fe-B phase diagram can be seen in Figure 2.  $\text{Fe}_2\text{B}$  can be grown out of an excess of Fe, cho-

\* Also at Physics Department, Gustavus Adolphus College

† vtaufour@ucdavis.edu

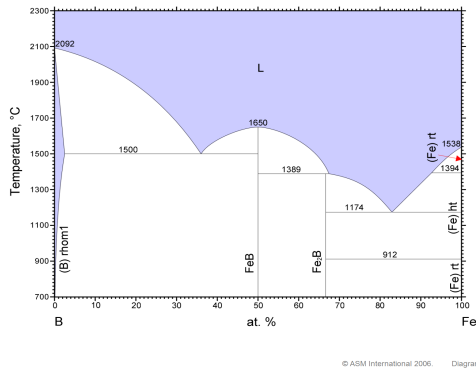


FIG. 2. The Fe-B binary phase diagram (After [3]).

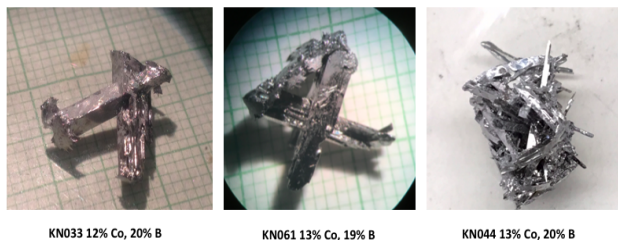


FIG. 3. Three crystals of  $(\text{Fe}_{1-x}\text{Co}_x)_2\text{B}$  produced by solution growth method with varying Co doping levels.

sen in this study as 19-20% B in 80-81% Fe. Levels of Co doping were chosen based on unpublished data as seen in Figure 1. Mixtures of Fe (99.98%), Co (99.9%, Alfa Aesar), and B (99.9%, Eagle Pitcher) pieces with appropriate stoichiometry were arc-melted together, placed in a crucible, and sealed into a quartz ampoule filled with 150 mm-Hg of argon gas. The ampoule was heated in a furnace to 1200°C for 5 hours where all materials were in a liquid phase. This was followed by an 80 hours cooling at a rate of -0.625°C/hour to 1150°C. Ampoules were spun in a centrifuge upon removal from the furnace at 1150°C to separate the liquid solution from the crystals. Several resulting crystals can be seen in Figure 3.

Some of the produced crystals were ground into a powder using a mortar and pestle and prepared for measurement using a Rigaku MiniFlex600 powder x-ray diffractometer. The resulting diffraction patterns are compared to known diffraction patterns using PDXL software to determine the sample contents.

Platinum leads of 0.002 inch diameter were attached to single rod-shaped crystals with H20E silver epoxy and soldered to a resistivity puck. Resistivity measurements were performed using a Quantum Design Physical Property Measurement System (PPMS) on two samples where  $x_{nominal} = 12.5\%$  over a range of temperatures from 1.8 to 300 K with no applied magnetic field.

Magnetization measurements on single crystals were performed using a Quantum Design superconducting quantum interference device magnetometer (MPMS). A

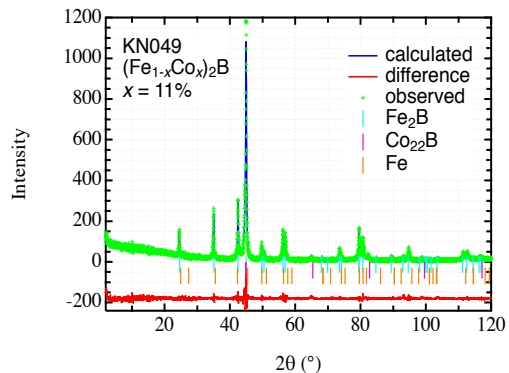


FIG. 4. Powder x-ray diffraction pattern for sample with  $x = 11\%$ . This figure includes indicators for peaks of  $\text{Fe}_2\text{B}$ ,  $\text{Co}_2\text{B}$ , and Fe, which make up the content of this sample.

crystal was placed between plastic straws and mounted to the end of the sample rod. Data were collected from 5 to 300 K under a 0.1 T magnetic field applied along or perpendicular to the c-axis to identify the presence of  $T_{sr}$  and its variance based on Co doping levels. Data were also collected with applied magnetic fields from 0 to 3 T. These magnetization versus applied field ( $\mu_0 H$ ) data were collected at temperatures near  $T_{sr}$  for  $x_{nominal} = 11\%$ . From this  $\Delta S_{iso}$  was calculated and the value of  $T_{sr}$  was determined.

### III. RESULTS AND DISCUSSION

Powder x-ray diffraction patterns were collected for various samples with  $x_{nominal} = 11 - 13\%$ . For sample with  $x_{nominal} = 11\%$ , analysis indicated that sample contents match known diffraction patterns with proportions of 74%  $\text{Fe}_2\text{B}$ , 16%  $\text{Co}_2\text{B}$ , and 10% Fe. This supports the expected results for  $(\text{Fe}_{1-x}\text{Co}_x)_2\text{B}$  crystals, which would match best to both  $\text{Fe}_2\text{B}$  and  $\text{Co}_2\text{B}$ . The diffraction pattern for the sample of  $x_{nominal} = 11\%$  can be seen in Figure 4.

Resistivity measurements were made using a PPMS for a sample of  $x_{nominal} = 12.5\%$  crystal. Results are seen in Figure 5. This curve is consistent with metallic behaviors that include a linear relationship between resistivity and temperature at high temperatures, a quadratic relationship at low temperatures, and small absolute values of  $\rho$ . The residual resistance ratio (RRR) has a value of 5. Such a rather small value is consistent with the Fe-Co substitution disorder.

The spin reorientation in  $(\text{Fe}_{1-x}\text{Co}_x)_2\text{B}$  can be observed from MPMS data. Figure 6 gives an example of such data. In this figure a crystal of  $x_{nominal} = 12\%$  has its largest magnetization at high temperature and applied field along the c-axis and its smallest magnetization at high temperature and applied field perpendicular to the c-axis. The change between high and low magnetization is gradual. These results are reproducible for

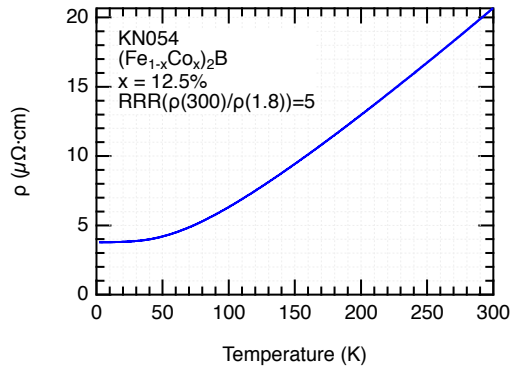


FIG. 5. Resistivity measurements of  $(\text{Fe}_{1-x}\text{Co}_x)_2\text{B}$  sample KN054 with  $x_{\text{nominal}} = 12.5\%$ . Measurements made using Quantum Design PPMS with no applied field and a temperature range between 1.8 K and 300 K. The shape of the curve and absolute values indicate  $(\text{Fe}_{1-x}\text{Co}_x)_2\text{B}$  alloys are metallic.

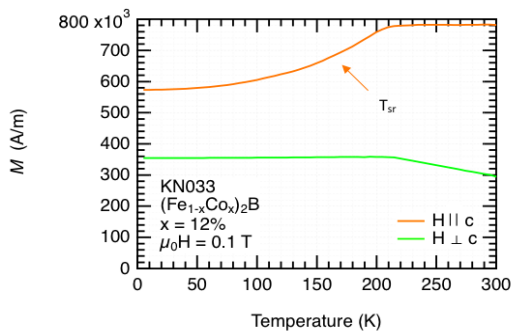


FIG. 6. Change in magnetization as temperature is varied for sample of  $x_{\text{nominal}} = 12\%$ . Opposite behaviors are observed between applied fields parallel and perpendicular to the  $c$ -axis. The  $T_{sr}$  of this sample is selected as the inflection point when  $H||c$  as indicated above.

crystals between  $x_{\text{nominal}} = 11\%$  and  $x_{\text{nominal}} = 13\%$  with varying shifts in transition temperatures.

$T_{sr}$  is tunable in  $(\text{Fe}_{1-x}\text{Co}_x)_2\text{B}$  by  $x$ . Transitions between 0 and 300 K were observed for  $x_{\text{nominal}} = 11\text{--}13\%$ . Crystals with  $x_{\text{nominal}} = 11\%$  have the highest transition temperature while crystals with  $x_{\text{nominal}} = 13\%$  have the lowest transition temperature. Samples of  $x_{\text{nominal}} > 13\%$  do not have transitions in the range of 5 to 300 K. The value of  $T_{sr}$  was estimated for measured samples using  $H||c$  curves and finding the inflection points on each  $H||c$  curve. These values were added to unpublished data seen in Figure 1. The relationship between temperature and Co content is linear in both unpublished data and data from this study.

Near the spin reorientation temperature, an inverse magneto-caloric effect is observed. This effect is observed as a positive change in entropy when the field is applied along the  $c$ -axis. This differs from a magneto-caloric ef-

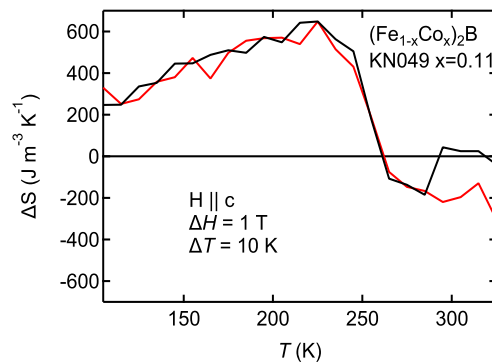


FIG. 7. Inverse magneto-caloric effect observed as a change in entropy as a function of temperature for two  $x_{\text{nominal}} = 11\%$   $(\text{Fe}_{1-x}\text{Co}_x)_2\text{B}$  samples. This effect occurs gradually below 250 K.

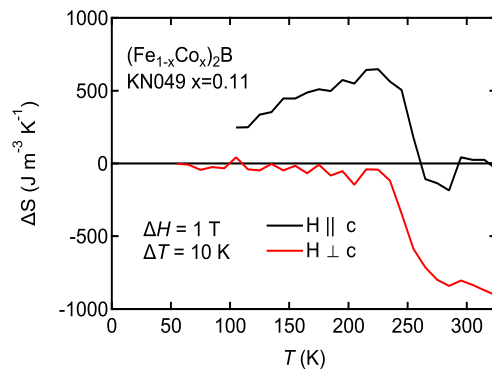


FIG. 8. Inverse magneto-caloric effect observed as a change in entropy as a function of temperature for  $x_{\text{nominal}} = 11\%$   $(\text{Fe}_{1-x}\text{Co}_x)_2\text{B}$  sample when  $H||c$ . No effect is observed when  $H \perp c$ .

fect which would result in a negative change in entropy when field is applied. From MPMS data of magnetization versus applied field,  $\Delta S_{iso}$  was calculated by

$$\Delta S_{iso}(T, \Delta H) = \frac{\mu_0}{T_u - T_l} \int_{H_i}^{H_f} [M(T_u, H) - M(T_l, H)] dH$$

where  $T$  is temperature,  $M$  is the magnetization, and  $\mu_0 H$  is applied magnetic field. The result is seen in Figure 7 for a  $(\text{Fe}_{1-x}\text{Co}_x)_2\text{B}$  sample of  $x_{\text{nominal}} = 11\%$ . The positive change in entropy occurs at temperatures less than 250 K. The change in entropy gradually increases as temperature is increased as expected due to the gradual change in magnetization as seen in Figure 6. As seen in Figure 8, when  $H \perp c$ , no magneto-caloric effect is observed. The gradual inverse magneto-caloric effect, sharp decline after 250 K, and unmeasured effect when  $H \perp c$  is most likely attributed to a demagnetization effect. This effect results in a reduction of magnetization relating to the shape of each sample. Future studies will be done with samples of different dimensions to further understand this effect.

#### IV. CONCLUSIONS

The directional dependence of magnetic properties was studied in single crystals of  $(\text{Fe}_{1-x}\text{Co}_x)_2\text{B}$ . These single crystals were produced by a solution growth method for Co doping between 11-17%.  $(\text{Fe}_{1-x}\text{Co}_x)_2\text{B}$  crystals exhibited spin reorientation transition temperatures between 5 and 300 K when  $x_{\text{nominal}} = 11 - 13\%$  that were estimated from magnetization versus temperature data when  $H||c$ . Near the spin reorientation temperature, an inverse magneto-caloric effect was observed at  $x_{\text{nominal}} = 11\%$ . No magneto-caloric effect was observed when  $H \perp c$ . Further work is being done to measure the  $\Delta S_{\text{iso}}$  for samples where  $x_{\text{nominal}} > 11\%$  with the magnetic field applied parallel and perpendicular to the c-axis and to understand the limitations due to the demagnetization effect.

#### V. ACKNOWLEDGEMENTS

We acknowledge the financial support of the University of California, Davis Physics Research Experience for Undergraduates program from the National Science Foundation grant PHY-1560482.

Thank you, Valentin, for sharing your enthusiasm for this project and your lab. Your kindness was greatly appreciated in addition to the knowledge and skills you taught me. Many thanks to Peter, Jackson, Jeff, and Hanshang for sharing their research expertise and for their time and patience while helping me.

Thank you, Rena, for your time and efforts to provide valuable information and enjoyable experiences throughout the summer. Thank you, REU students, for adding to this experience.

- 
- [1] A.M. Tishin and Y.I. Spichkin, *The Magnetocaloric Effect and Its Applications* (IOP Publishing, London, 2003).  
 [2] J.J. Ipus *et al.*, *J. Magn. Magn. Mater.* **436** (2017).  
 [3] P.K. Liao and K.E. Spear, *Binary Alloy Phase Diagrams*,

- ASM Handbooks. **2** (1990).  
 [4] V. Taufour, *unpublished*.